THE JOURNAL OF BIOLOGICAL CHEMISTRY VOL. 283, NO. 16, pp. 10632–10641, April 18, 2008
© 2008 by The American Society for Biochemistry and Molecular Biology, Inc. Printed in the U.S.A.

Repetitive Firing Triggers Clustering of Kv2.1 Potassium Channels in *Aplysia* Neurons*

Received for publication, January 10, 2008, and in revised form, February 13, 2008 Published, JBC Papers in Press, February 13, 2008, DOI 10.1074/jbc.M800253200

Yalan Zhang[‡], **Sharen E. McKay**[§], **Benoit Bewley**[‡], **and Leonard K. Kaczmarek**[‡1]

From the Departments of [‡]*Pharmacology and* [§]*Pathology, Yale School of Medicine, New Haven, Connecticut 06520*

The *Kv2.1* gene encodes a highly conserved delayed rectifier potassium channel that is widely expressed in neurons of the central nervous system. In the bag cell neurons of *Aplysia*, Kv2.1 channels contribute to the repolarization of action potentials during a prolonged afterdischarge that triggers a series of reproductive behaviors. Partial inactivation of *Aplysia* Kv2.1 during repetitive firing produces frequency-dependent broadening of action potentials during the afterdischarge. We have now found that, as in mammalian neurons, Kv2.1 channels in bag cell neurons are localized to ring-like clusters in the plasma membrane of the soma and proximal dendrites. Either elevation of cyclic AMP levels or direct electrical stimulation of afterdischarge rapidly enhanced formation of these clusters on the somata of these neurons. In contrast, injection of a 13-amino acid peptide corresponding to a region in the C terminus that is required for clustering of Kv2.1 channels produced disassociation of the clusters, resulting in a more uniform distribution over the somata. Voltage clamp recordings demonstrated that peptide-induced dissociation of the Kv2.1 clusters is associated with an increase in the amplitude of delayed rectifier current and a shift of activation toward more negative potentials. In current clamp recording, injection of the unclustering peptide reduced the width of action potentials and reduced frequency-dependent broadening of action potentials. Our results suggest that rapid redistribution of Kv2.1 channels occurs during physiological changes in neuronal excitability.

The Kv2.1 voltage-dependent potassium channel subunit is expressed in a wide range of neurons in the mammalian central nervous system. In heterologous expression systems, Kv2.1 usually produces potassium currents that activate and inactivate relatively slowly (1–4). It has been suggested that activation of Kv2.1 channels occurs primarily during repetitive stimulation of neurons, leading to a decrease in excitability during such stimulation (4, 5).

A series of studies by Trimmer and co-workers (5) have demonstrated that Kv2.1 channels have an unusual distribution in the plasma membrane and that this localization can be modified by neuronal activity. In cortical and hippocampal neurons, Kv2.1 is localized to numerous discrete clusters on the soma and proximal dendrites. It has been proposed that Kv2.1 channels regulate the spread of excitation between the soma and distal dendrites of these neurons. The Kv2.1 clusters are typically circular or "donut"-shaped. Several forms of neuronal stimulation can, however, eliminate this pattern of channel localization. The induction of seizure activity or the application of glutamate or muscarinic agonists to isolated neurons produces dissolution of the clusters leading to a more uniform distribution of Kv2.1 immunoreactivity in the plasma membrane (5). This alteration in channel location can be attributed to stimulation-induced elevation of calcium levels, which activates a calcium-dependent phosphatase, leading to the dephosphorylation of Kv2.1 at sites located in its cytoplasmic C terminus (6). Dephosphorylation of Kv2.1 also produces hyperpolarizing shifts in the voltage dependence of activation and inactivation (5, 6).

Kv2.1 is an ortholog of the *Shab* gene in *Drosophila* (7), and orthologs of these channels have been cloned and characterized in a wide range of vertebrate and invertebrate species. Although the sequence of these channels has been relatively highly conserved across evolution, their specific electrical characteristics are not so well conserved. For example, the homolog of Kv2.1 in the marine mollusk *Aplysia californica*, differs from the mammalian channel in a number of ways. In this species, neuronal action potentials can be relatively broad (>10–200 ms), and activation of *Aplysia* Kv2.1 occurs rapidly enough to contribute to the repolarization of individual action potentials (8). Moreover, in contrast to mammalian Kv2.1, which inactivates very slowly with maintained depolarization (over ~3–5 s), *Aplysia* Kv2.1 inactivates within several hundred milliseconds. Repetitive depolarization of the *Aplysia* channel at frequencies greater than ~1 Hz produces cumulative inactivation, leading to frequency-dependent broadening of action potentials at firing rates greater than 1 Hz (8, 9).

The clustering of mammalian Kv2.1 channels can be attributed to a 26-amino acid targeting sequence located in the proximal cytoplasmic C-terminal domain of the channel (10). Four residues within this region are critical for localization to clusters. A conserved clustering sequence can be found in the C-terminal domain of *Aplysia* Kv2.1. The *Aplysia* sequence differs from that in rat or humans, however, in that a unique cAMP-dependent protein kinase phosphorylation site is located within the *Aplysia* clustering sequence (8).

The *Aplysia* Kv2.1 channel is expressed in the bag cell neurons within the abdominal ganglion. These neurons have been used extensively to investigate the mechanisms of prolonged changes in the intrinsic excitability of neurons following brief synaptic stimulation (11, 12), as well mechanisms of neuropeptide synthesis and secretion (13–15). In response to very brief

* The costs of publication of this article were defrayed in part by the payment of page charges. This article must therefore be hereby marked "*advertisement*" in accordance with 18 U.S.C. Section 1734 solely to indicate this fact.

[1] To whom correspondence should be addressed: Dept. of Pharmacology, Yale School of Medicine, 333 Cedar St., New Haven, CT 06520. Tel.: 203-785-4500; Fax: 203-785-5494; E-mail: leonard.kaczmarek@yale.edu.

This is an Open Access article under the CC BY license.

stimulation of an input, these neurons generate a ~30-min period of repetitive firing, termed the "afterdischarge," which causes the secretion of several neuroactive peptides. During this afterdischarge cyclic AMP levels are elevated, producing an increase in action potential broadening (9, 16). This allows action potentials that are generated at distal sites in the neurites to progressively invade the proximal neurites and somata of the bag cell neuronal network (16, 17). At the end of the afterdischarge, the neurons enter a prolonged (~18 h) refractory state, during which further stimulation fails to evoke afterdischarges. This pattern of electrical activity allows these neurons to act as a "master switch" for a series of reproductive behaviors.

In this paper we have examined the localization of *Aplysia* Kv2.1 channels. We have found that, like mammalian Kv2.1, *Aplysia* Kv2.1 channels form clusters in the plasma membrane at the soma and proximal dendrites of bag cell neurons. Physiological stimulation of an afterdischarge or elevation of cyclic AMP levels produces an increase in cluster formation. We have also found that clusters can be dissolved by injection of a peptide corresponding to the clustering sequence within the C terminus and that this is associated with an increase in potassium current that serves to prevent frequency-dependent action potential broadening. Our findings suggest that formation and dissolution of Kv2.1 clusters is an evolutionarily conserved mechanism that regulates propagation of information toward and through the somata of neurons.

EXPERIMENTAL PROCEDURES

Animals and Cell Culture—Adult *A. californica* weighing 100–200 g were obtained from Marine Specimens Unlimited (San Francisco, CA) or Marinus Inc. (Long Beach, CA). The animals were housed in an ~400-liter aquarium containing continuously circulating, aerated Instant Ocean (Aquarium Systems, Mentor, OH) salt water at 14 °C on an ~12-h light/dark cycle and were fed Romaine lettuce three times a week. All of the experiments were performed at room temperature (18–20 °C).

For primary cultures of isolated bag cell neurons, the animals were anesthetized by an injection of isotonic $MgCl_2$ (~50% of body weight); the abdominal ganglion was removed and treated for 18 h at 18–20 °C with neutral protease (13.33 mg/ml; 165859; Roche Applied Science) dissolved in normal artificial seawater (nASW).[2] nASW was composed of 460 mM NaCl, 10.4 mM KCl, 11 mM $CaCl_2$, 55 mM $MgCl_2$, 15 mM HEPES, 1 mg/ml glucose, 100 units/ml penicillin, and 0.1 mg/ml streptomycin; pH was adjusted to 7.8 with NaOH. The ganglion was then transferred to fresh nASW, and the bag cell neuron clusters were dissected from their surrounding connective tissue. Using a fire-polished Pasteur pipette and gentle trituration, the neurons were dispersed in nASW onto 35 × 10-mm polystyrene tissue culture dishes (no. 25000; Corning, Corning, NY). The cultures were maintained in nASW for 1–3 days in a 14 °C incubator. For all of the experiments using isolated neurons in this study, the number of observations (*n*) refers to number of cells, and the experiments were always carried out using cultures prepared from at least two to four different animals.

In experiments to test the effects of afterdischarge on the distribution of Kv2.1 immunoreactivity, intact abdominal ganglia together with bag cell clusters and their pleuroabdominal connective nerves were first incubated for 18 h with neutral protease to soften the collective tissue exactly as described above. The ganglia were then placed in a recording chamber, and afterdischarges were evoked by a stimulus train (20V, 2.5 ms, 6 Hz, 15 s) applied to a suction electrode on the connective nerve. The discharges were monitored through a second suction electrode over the bag cell clusters. Thirty minutes after stimulation, the clusters were dissociated into isolated cells as described above and were then fixed for immunocytochemistry 45 min after stimulation.

Establishment of Aplysia Kv2.1 Stable Cell Line—The *Aplysia* Kv2.1 clone in Bluescript was subcloned into the mammalian expression vector pcDNA3 and used to transfect Chinese hamster ovary (CHO) cells. CHO cells were grown in Iscove's medium with 10% fetal calf serum, penicillin, streptomycin, and hypoxanthine supplement. Stable cell lines were generated via Lipofectamine 2000-mediated transfection using geneticin as a selection agent for transfected cells. Once the transfected cells had grown to near confluence, the cells were trypsinized, resuspended in medium with low serum, and sorted by size and nuclear refractance so that dead cells were removed, and individual live cells were plated in isolation to create colonies of transfected cells derived from a single progenitor (Yale Cancer Center FACS Center). The colonies were grown to confluence and then plated in 35-mm dishes and assayed for the presence of *Aplysia* Kv2.1 channels by recording the whole cell current response to a voltage step to +20 mV with the membrane potential clamped at −70 mV with a gigaohm resistance at the electrode-cell junction (whole cell patch clamp mode). Five positive colonies were isolated, and all showed an inactivating voltage-dependent outward current with conductance-voltage relationships similar to that described by Quattrocki *et al.* (8) for *Aplysia* Kv2.1 in oocytes.

Antibody Production and Purification—The peptides were synthesized to generate antibodies against amino acid sequences encoded by the cloned *Aplysia* Kv2.1 cDNAs (GenBank™ accession number S68356). The peptide (C*X*DRADPSLNQDNE), which includes 12 amino acids in the extracellular region between S1 and S2, was synthesized at the W. M. Keck Biotechnology Resource Center at Yale University. The *X* represents aminocaproic acid, which acted as a spacer molecule between the specific sequence and a nonspecific N-terminal cysteine, which allowed conjugation of the peptide to bovine serum albumin. Bovine serum albumin, in turn, acted as a carrier for antigenic peptide in the generation of chicken polyclonal IgY, which was carried out by Aves Labs, Inc. (Tigard, OR). For affinity purification of IgYs, the synthetic peptides were conjugated to Sulfolink Coupling Gel (Pierce) by the N-terminal cysteine. Each of the two prepared columns was incubated with IgYs for 1 h at room temperature, and then the columns were washed three times with phosphate-buffered saline (PBS). Specific antibodies were eluted with a 100 mM glycine buffer, pH 2.5, and then immediately neutralized with 1

[2] The abbreviations used are: nASW, normal artificial seawater; CHO, Chinese hamster ovary; PBS, phosphate-buffered saline; FITC, fluorescein isothiocyanate; 8-CPT-cAMP, 8-(4-chlorophenythio)-cAMP.

M Tris, pH 8.5. Fractions containing proteins (measured by the optical density at 280 nm) were pooled and dialyzed against PBS using Slide-A-Lyzer cassettes (Pierce) and concentrated using a spin column.

Immunoprecipitation—Stably transfected CHO cells were lysed with standard radioimmune precipitation assay buffer containing Complete protease inhibitor (Roche Applied Science). The lysate was precleared with goat anti-IgY immobilized on agarose beads. Kv2.1 was immunoprecipitated from the lysate using affinity-purified chicken anti-Kv2.1 or a fraction of the column flow (nonimmune) through IgY as a control. Following incubation with IgY, the immobilized goat anti-IgY was used to concentrate the IgY-Kv2.1 complexes, and then the pellet was resuspended in SDS gel loading buffer with β-mercaptoethanol and separated on a 4–15% gradient gel (Bio-Rad). The gel was stained with 0.01% silver nitrate.

Immunoblotting—Bag cell neuron clusters were dissected from 200–250-g animals. The clusters were homogenized in 100 μl of buffer (1% Lubrol, 50 mM Tris-HCl, pH 7.4, 10 nM sodium orthovanadate, 30 mM sodium pyrophosphate, 50 mM NaF, 20 μM $ZnCl_2$, 0.25 mM phenylmethylsulfonyl fluoride, containing protease inhibitor mixture; Roche Applied Science) in glass-glass tissue grinders for 3 min on ice. The samples were then centrifuged at 5,000 $\times$ *g* for 20 min. The supernatants were collected and transferred to 1.5-ml Eppendorf tubes. SDS gel-electrophoresed proteins were transferred to a immunoblot polyvinylidene difluoride membrane (Bio-Rad). Nonspecific binding was blocked by incubating the blot in Tris-buffered saline Tween 20 (TBST) buffer with 5% milk for 1 h at room temperature. The blots were incubated with anti-APKv2.1 antibody (1: 200) developed in chicken or with primary antibody incubated with excess antigen peptide overnight at 4 °C and then washed four times for 30 min each, followed by application of secondary antibodies (horseradish peroxidase-linked anti-chicken Ig Y; Pierce) at 1:10,000 dilution for 1 h at room temperature. After three washes of 30 min each in TBST, immunoreactive proteins were visualized with detection reagent (Amersham Biosciences).

Immunocytochemistry and Confocal Microscopy—Staining of cultured bag cell neurons was performed on coverslips coated with 1 μg/ml poly-D-lysine (Sigma). Bag cell neurons were cultured in nASW for 1–2 days before fixation with 4% paraformaldehyde in 400 mM sucrose/nASW, as described previously (18). Three ml of fixative solution were then rapidly superfused into the central well, and fixation was allowed to continue for 25 min. The culture dishes were then washed twice with phosphate-buffered saline (PBS) and blocked with 5% goat serum/PBS before incubation with primary antibodies. The coverslips were removed from the culture dishes, inverted on 100 μl of primary antibody solution, and placed in a humidified chamber at 4 °C overnight. The primary antibody was used at a dilution of 1:10,000 in 5% goat serum/PBS. After overnight incubation, the coverslips were washed extensively with PBS and then incubated for 2 h at room temperature with fluorescein or Cy3-conjugated goat anti-chicken IgG secondary antibodies (FITC-GαCigG or Cy3-GαCigG, Molecular Probes). The coverslips were washed and mounted on glass slides using mounting medium. The stained slides were viewed and photographed using Axiovision software (Zeiss). Measurements of relative fluorescence were made by converting the Axiovision files to TIFF files. Regions of interest were defined (4–25 μm^2) using Adobe Photoshop 7.0, and the relative luminosity for each region of interest was calculated. Confocal microscopy was carried out using a Zeiss LSM-510 confocal microscope.

Because of the large size of bag cell neurons (up to 80 μm in diameter), the focal planes corresponding to apical and basal surfaces of isolated bag cells neurons could readily be differentiated using two criteria. First, neurites and axons extend in length along the flat surface of the dish only at the basal surface of the cells and are generally not visible in sections of the apical surface. Second, during confocal imaging, we obtained three-dimensional projection images to establish the complete topology of the cells.

In confocal sections, the apical surface of each neuron was defined as the last apical section before a section in which no clear signal could be visualized, and in all cases, the cross-sectional area of this section was no smaller than 80% of the cross-sectional area of sections at the center of the cell. Individual clusters were defined as patches of immunostaining with a cross-sectional diameter of at least 1 μm. Because bag cell neurons are a homogenous population of neurons and because control and experimental cells were taken from the same animals, we quantified cluster number by counting the total number of patches at the apical surface of each control and experimental cell.

Localization of Kv2.1 in Tissue Sections—Tissue was dissected and fixed as described above. Following fixation the tissue was further cryoprotected and rinsed in PBS with 20% sucrose for 18–24 h at 4 °C before embedding in TissueTek medium and freezing in a slurry of acetone and dry ice. Twelve-micrometer sections were cut through the ganglia using a cryostat. The sections were collected on polylysine-coated slides, air dried briefly, and used for antibody staining immediately. The sections were blocked in 2% goat serum/PBS with 0.5% Triton X-100 for 1 h, incubated for 1 h in 2 μg/ml anti-*Aplysia* Kv2.1 in blocking solution, rinsed three times in PBS, incubated in 1/500 diluted goat anti-rabbit FITC-secondary for 1 h, rinsed again in PBS, and covered with a coverslip with Citifluor. The sections were viewed with a Nikon Optiphot light microscope and photographed with Kodak EliteChrome 400 slide film.

Injection of Anti-Aplysia Kv2.1 Peptide into Bag Cell Neurons—Bag cell neurons were isolated and maintained in primary culture according to the previously described method of Kaczmarek *et al.* (19). Current clamp and voltage clamp recordings were made from bag cell neurons using an AxonClamp 2B (Axon Instruments, Union City, CA). For current clamp recordings, the single sharp electrode, bridge balance method was used. For voltage clamp analysis, the discontinuous single-electrode approach was used (20, 21), in which the membrane potential is changed using a high frequency train of current pulses and measurements of membrane potential are made immediately prior to each current pulse. The discontinuous single electrode voltage clamp amplifier was run at a switching frequency of 1–2 kHz. To ensure adequate voltage control, the individual pulses were monitored on an oscilloscope and adjusted so that the period of voltage sampling corresponded to

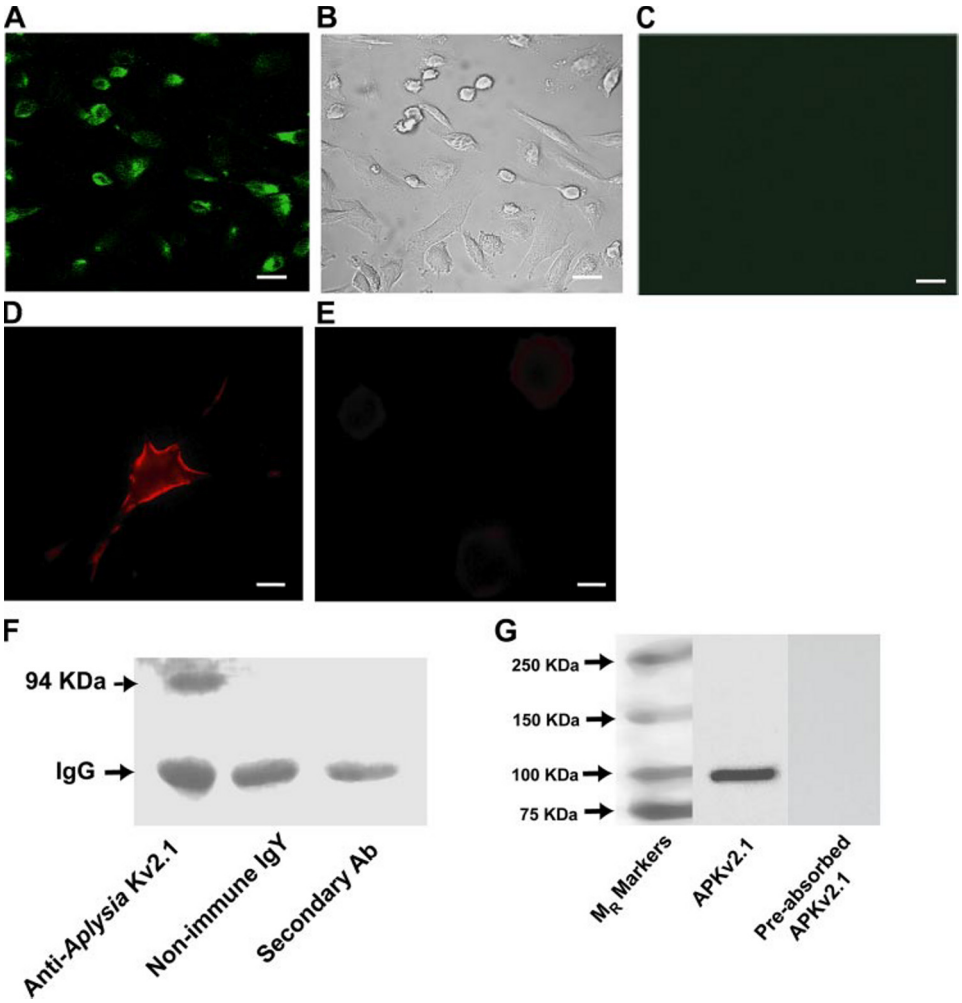

FIGURE 1. **Characterization of the *Aplysia* Kv2.1 antibody.** *A–C*, immunostaining of CHO cells transiently transfected with *Aplysia* Kv2.1 (*A*) or pTracer alone (*B*). *Scale bars*, 20 μm. *D* and *E*, immunostaining of cultured bag cell neurons with chicken anti-*Aplysia* Kv2.1 antibody. Fixed, nonpermeabilized bag cell neurons were immunostained using chicken anti-*Aplysia* Kv2.1 (*C*) or using the same antibody pretreated with *Aplysia* Kv2.1 peptide (*D*). A FITC-conjugated secondary antibody was used as described under "Experimental Procedures." *Scale bars*, 30 μm. *F*, silver-stained gel showing that chicken anti-*Aplysia* Kv2.1 antibody specifically immunoprecipitates a protein with a M_r of ~94 kDa from CHO cells transfected with the *Aplysia Kv2.1* gene (*left lane*). No band was detected with nonimmune IgY (IgY that was not absorbed by an affinity column containing the immunogen peptide (*center lane*) or with the secondary antibody alone (goat anti-IgY, (*right lane*)). *G*, immunoblot of proteins prepared from *Aplysia* abdominal ganglion and probed with the antibody against *Aplysia* Kv2.1 (*center lane*). The *right lane* demonstrates that no signal on Western blots could be observed when the anti-Kv2.1 antibody was preincubated overnight with the antigen peptide. The *left lane* shows molecular mass markers.

up to nine electrode time constants. Microelectrodes were pulled from borosilicate glass capillaries (1.2-mm ID, TW 120F-4; World Precision Instruments, Sarasota, FL) and had tip diameters of <1 μm and had resistances of ~2 MΩ when filled with 3 M KCl. The injections were made with pressure pulses (typically 1–10 pulses; each pulse ~100 ms in duration) using a Picospritzer (General Valve, Fairfield, NJ) and an injection pressure of 14 p.s.i. The injection solutions contained 11 mM Tris-HCl, pH 7.2, 530 mM potassium acetate, 4.3 mg/ml FITC or rhodamine dextran (to monitor injections), and peptide (5 μM). The voltage was filtered at 3 kHz using the Axonclamp built-in Bessel filter and sampled at 2 kHz using a Digidata 1322A A/D converter (Axon Instruments), an IBM-compatible personal computer, and Clampex. All of the current clamp recordings were performed in nASW. Current was delivered with Clampex software (version 8.2; Axon Instruments). For voltage clamp recordings, the $CaCl_2$ in nASW was replaced by 2 mM $CoCl_2$, and the holding potential is at -40 mV. For staining, the cells were fixed within 60 min after injection.

Computer Simulations—Simulations of the effects *Aplysia* Kv2.1 current on action potential broadening were carried out using the following equation,

$$C dV/dt = g_{Ca} n^3 j(50 - V) + g_{K1} m^3 h(-80 - V) + g_{K2} p(-80 - V) + g_L(E_{rest} - V) + Is \quad \text{(Eq. 1)}$$

where g_{K1} describes the value of the *Aplysia* Kv2.1 conductance. This equation is similar to that used previously to describe the effects of *Aplysia* Kv2.1 on action potentials of bag cell neurons (8) except for the addition of a second voltage-dependent potassium conductance (g_{K2}) governed by the gating variable p, which evolved according to equations identical in form to Equations 2–4 of Ref. 8. All of the parameters were identical to those of described by Quattrocki *et al.* (8) with the exception of $g_{Ca} = 0.8$ μs, $E_{rest} = -60$ mV and with the following parameters for the evolution of the variable p: $g_{K2} = 0.05$ μs, $u_p = 0.1$ mV^{-1}, $A_p = 0.141$ ms^{-1}, and $w_p = 0.021$ mV^{-1}. In Fig. 8*A*, the control value of the *Aplysia* Kv2.1 conductance g_{K1} was 1.5 μs and was raised to 1.8 μs in the *center panel*. For the *right-hand panel* in Fig. 8 showing the effects of altered voltage dependence, g_{K1} was 1.5 μs, but V_m was changed from -10 to -20 mV.

RESULTS

Characterization of the Anti-Aplysia Kv2.1 Antibody—To examine the localization of *Aplysia* Kv2.1 in bag cell neurons, we generated antibodies in chicken against a synthetic peptide containing a 12-amino acid sequence corresponding to the extracellular loop between the S1 and S2 hydrophobic segments of the channel (8). Characterization of this antibody was first carried out by immunostaining CHO cells transiently transfected with the *Aplysia Kv2.1* gene. Such transfected cells were strongly labeled with this anti-*Aplysia* Kv2.1 antibody (Fig. 1*A*). In contrast, no staining was detected in CHO cells transfected with the vector alone (Fig.

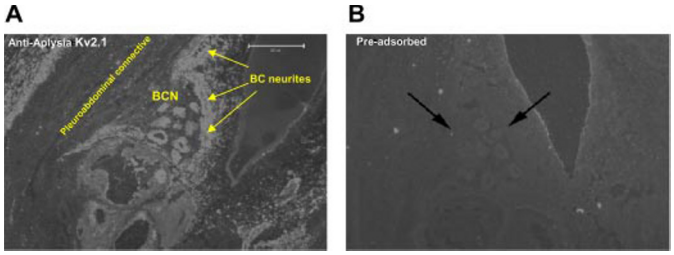

FIGURE 2. **Immunostaining of tissue sections through the abdominal ganglion with chicken *Aplysia* Kv2.1 antibody.** Neighboring 12 μM cryostat sections through the abdominal ganglion, including one bag cell cluster, were probed with chicken anti-*Aplysia* Kv2.1 antibody and then stained with an FITC-conjugated secondary antibody (*A*). The cluster of bag cell neuron somata is indicated (*BCN*) as are the underlying pleuroabdominal connective nerve and the location of the bag cell neurites (*BC neurites*) that extend over the cluster of somata and along the peripheral edge of the pleuroabdominal connective. Staining of some other neurons in the body of the abdominal ganglion can also be detected. *Scale bar*, 200 μm. No staining was detected with peptide preincubation before primary antibody (*B*). The *black arrows* indicate the positions of bag cell somata.

1*C*). The chicken anti-*Aplysia* Kv2.1 antibody specifically immunoprecipitated a protein of ~ 94 kDa from homogenates of CHO cells transfected with the *Aplysia Kv2.1* (Fig. 1*F*). A band of the same molecular mass was also detected on Western blots of preparations from abdominal ganglia of *Aplysia* (Fig. 1*G*), and no band was detected when the antibody was preabsorbed overnight with the antigen peptide prior to immunoblotting.

Distribution of Aplysia Kv2.1 Channels in Cultured Bag Cell Neurons and in Intact Abdominal Ganglia—To examine the cellular localization of *Aplysia* Kv2.1 in bag cell neurons in more detail, we prepared cultures of isolated neurons (19). Fig. 1*D* shows a confocal image through the center of the soma of an isolated neuron stained with anti-*Aplysia* Kv2.1. Dense clusters of immunoreactivity were detected at the edge corresponding to the plasma membrane of the soma. Less intensely stained clusters could also be seen on the proximal neurites. No immunostaining could be detected when the antibody was preincubated with the immunogen peptide (Fig. 1*E*).

We also examined the localization of *Aplysia* Kv2.1 in the intact nervous system. Immunostaining of 12-μm cryostat sections through the abdominal ganglion confirmed that *Aplysia* Kv2.1 is strongly expressed in bag cell neurons, which are located in two clusters at the rostral end of the ganglion (Fig. 2*A*). Staining could also be detected in other cells of the ganglion. As for the isolated cells, no staining was observed when the antibody was preabsorbed with the immunogen peptide (Fig. 2*B*). Immunoreactivity for *Aplysia* Kv2.1 could be located both at the somata of individual bag cell neurons and in proximal neurites, which extend around the clusters of somata and around the pleuroabdominal connective nerve close to the abdominal ganglion. This general distribution exactly matches that for other markers of bag cell neuronal processes, such as egg laying hormone, their major neuropeptide transmitter (22).

Stimulation of Afterdischarge Increases Clustering of Kv2.1—The onset of afterdischarge in bag cell neurons is associated with an elevation of cyclic AMP levels (16, 23, 24), which produce a reduction in the amplitude of voltage-dependent potassium current measured in voltage clamp experiments (25, 26). We tested the effect of elevating cyclic AMP levels on the distribution of Kv2.1 channels in bag cell neurons by exposing isolated cultured neurons to the membrane-permeant, phosphodiesterase-resistant cyclic AMP analog 50 μM 8-chlorophenythio-cAMP (8-CPT-cAMP) for 1 h. At this time, treated and untreated cells were fixed for immunocytochemistry. Treatment with 8-CPT-cAMP produced a clear increase in the number of discrete clusters of Kv2.1 immunoreactivity on the surface of the soma (Fig. 3*A*). This was quantified by counting the number of clusters that could be detected when focusing on the exposed apical surface of isolated cells, revealing that 50 μM 8-CPT-cAMP produced an ~2-fold increase in cluster number ($p < 0.0008$; Fig. 3*B*).

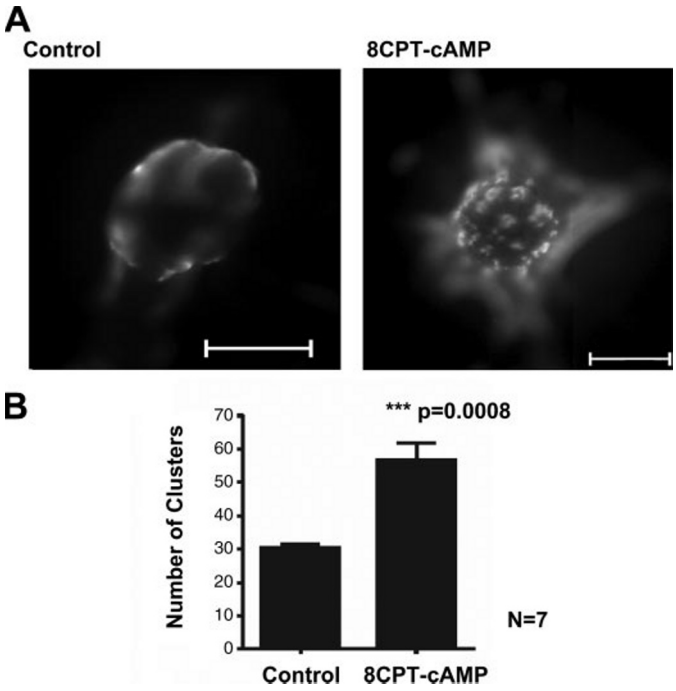

FIGURE 3. **Treatment of isolated bag cell neuron with a cyclic AMP analog increases the number of *Aplysia* Kv2.1 clusters on the apical surface of soma.** *A*, cultured bag cell neurons were incubated with 50 μM 8CPT-cAMP for 1 h (*right panel*) or left untreated (*left panel*). The cells were then fixed and stained for chicken *Aplysia* Kv2.1. The clusters were imaged using a conventional fluorescence microscope focused on the apical surface of the cells. *Scale bar*, 50 μm. *B*, quantification of the number of Kv2.1 channel clusters at the apical membrane surface of bag cell neurons incubated for 60 min in the presence or absence of 50 μM 8CPT-cAMP. The number of clusters with an area greater than 1 μm^2 was determined for the two groups. The data are expressed as the means ± S.E.

We also tested the effect of direct stimulation of afterdischarge in bag cell neurons on the distribution of Kv2.1 immunoreactivity. Intact abdominal ganglia together with bag cell clusters and their pleuroabdominal connective nerves were first incubated for 18 h in a solution containing neutral protease to soften the collective tissue. The ganglia were then placed in a recording chamber and suction electrodes were placed over the bag cell clusters and the distal connective nerve for recording and stimulation, respectively (Fig. 4*A*). Afterdischarge in the bag cell neurons were evoked by a stimulus train (20 V, 2.5 ms, 6 Hz, 15 s) applied to the connective nerve. Thirty minutes after stimulation, the clusters were dissociated into isolated cells, which were then fixed for immunocytochemistry 45 min after stimulation. Comparison with clusters that had not been stimulated to afterdischarge, using both visual inspection and quan-

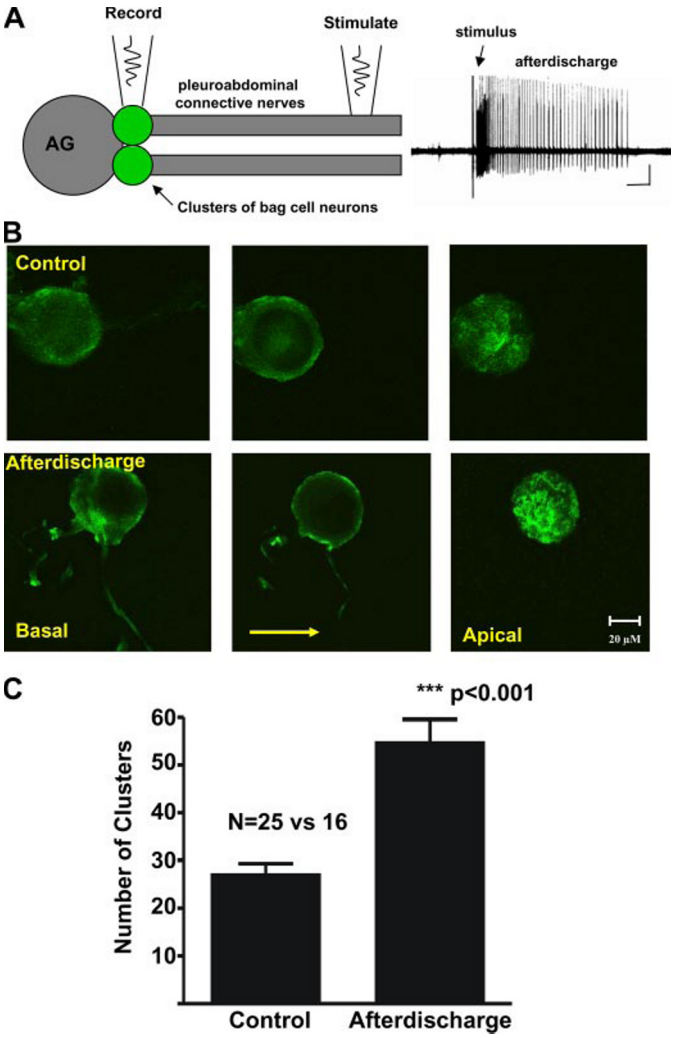

FIGURE 4. **Afterdischarge in bag cell neurons increases Kv2.1 clustering.** *A*, schematic diagram of an abdominal ganglion (*AG*) with two associated clusters of bag cell neurons (*left panel*). The placement of electrodes on one cluster and along the pleuroabdominal connective nerve is shown. The *right panel* shows an extracellular recording of the onset of an afterdischarge in response to a brief stimulus at arrow (20V, 2.5 ms, 6 Hz, 15 s) *Scale bars*, 3 min, 250 μV. *B*, confocal immunofluorescence staining for *Aplysia* Kv2.1 in an isolated neuron taken from a control clusters (*top row*) and one that had been stimulated to afterdischarge and fixed 45 min after stimulation (*bottom row*). For each cell, three confocal sections are shown at different levels, including the apical surface of the neuron (*right panels*). *C*, quantification of the number of Kv2.1 channel clusters at the apical membrane surface of bag cell neurons isolated from control ganglia and those in which the neurons had been stimulated to afterdischarge. Data are expressed as the mean ± S.E.

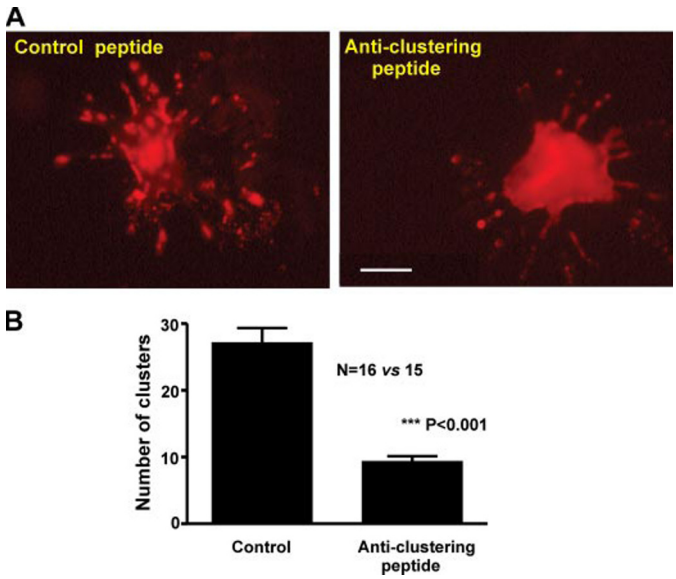

FIGURE 5. **The effect of injecting anti-clustering peptide into isolated bag cell neurons.** *A*, in control cells (control peptide-injected), Kv2.1 clusters, imaged with a conventional fluorescence microscope, are expressed on the soma and neurites of cultured bag cell neurons (*left panel*). The *right panel* shows the distribution of Kv2.1 immunoreactivity in a neuron injected with the anti-clustering peptide. The cells were fixed 60 min after peptide injection. *Scale bar*, 20 μm. *B*, quantification of the number of Kv2.1 channel clusters at the apical membrane surface of control bag cell neurons and those injected with the anti-clustering domain peptide. The number of clusters with an area greater than 1 μm^2 was counted in the two groups. The data are expressed as the means ± S.E.

tification of the numbers of Kv2.1-immunopositive clusters at the apical surface of the soma, revealed that the stimulation of afterdischarge produced a greater than 2-fold increase in the number of channel clusters on apical bag cell neuron membranes ($p < 0.001$, $n = 25$ *versus* 16; Fig. 4, *B* and *C*).

Synthetic Anti-clustering Peptide Reduces Clustering of Kv2.1 Channels—The localization of rat Kv2.1 channels to discrete clusters has been found to depend on a novel 26-amino acid targeting signal within the C-terminal cytoplasmic region (10). This targeting signal is conserved in *Aplysia* Kv2.1. To examine the potential consequences of clustering and declustering during the changes in excitability produced by stimulation of bag cell neurons, we synthesized a peptide (KRTGSIVSFHSIN) that corresponds to the central part of the clustering sequence of *Aplysia* Kv2.1 and that contains all four residues that have been found to be critical for localization to clusters (10). Such a peptide may be expected to interact with and displace the endogenous target of this sequence in Kv2.1 channels in native neurons. Control and experimental cultured bag cell neurons were penetrated with microelectrodes filled with 5 μM anti-clustering peptide or a control peptide with the sequence (CXDRADPSLNQDNE), which corresponds to the 12 amino acids of the S1-S2 region. FITC was included for visualization of the extent of injection by fluorescence microscopy. Sixty minutes after pressure injection into the soma (1–10 pulses 100 ms, 14 p.s.i.), the cultured neurons were fixed without permeabilization and processed for immunolocalization of the extracellular epitope of Kv2.1. Injection of the anti-clustering peptide produced a greater than 50% reduction in the density of clusters detected at the apical surface of the soma when compared with control cells (Fig. 5).

Anti-clustering Peptide Increases Potassium Currents and Reduces Frequency-dependent Action Potential Broadening—To determine whether the dissolution of surface Kv2.1 clusters produced by injection of the anti-clustering peptide is associated with changes in the potassium current or pattern of firing of action potentials, we carried out both voltage clamp and current clamp recordings of isolated cultured bag cell neurons before and after injection of the peptide.

In voltage clamp experiments, the holding potential was held at −40 mV to inactivate A currents (26), and 600-ms voltage commands were applied in 10-mV increments up to +50 mV. Because a holding potential of −40 mV produces less than 20%

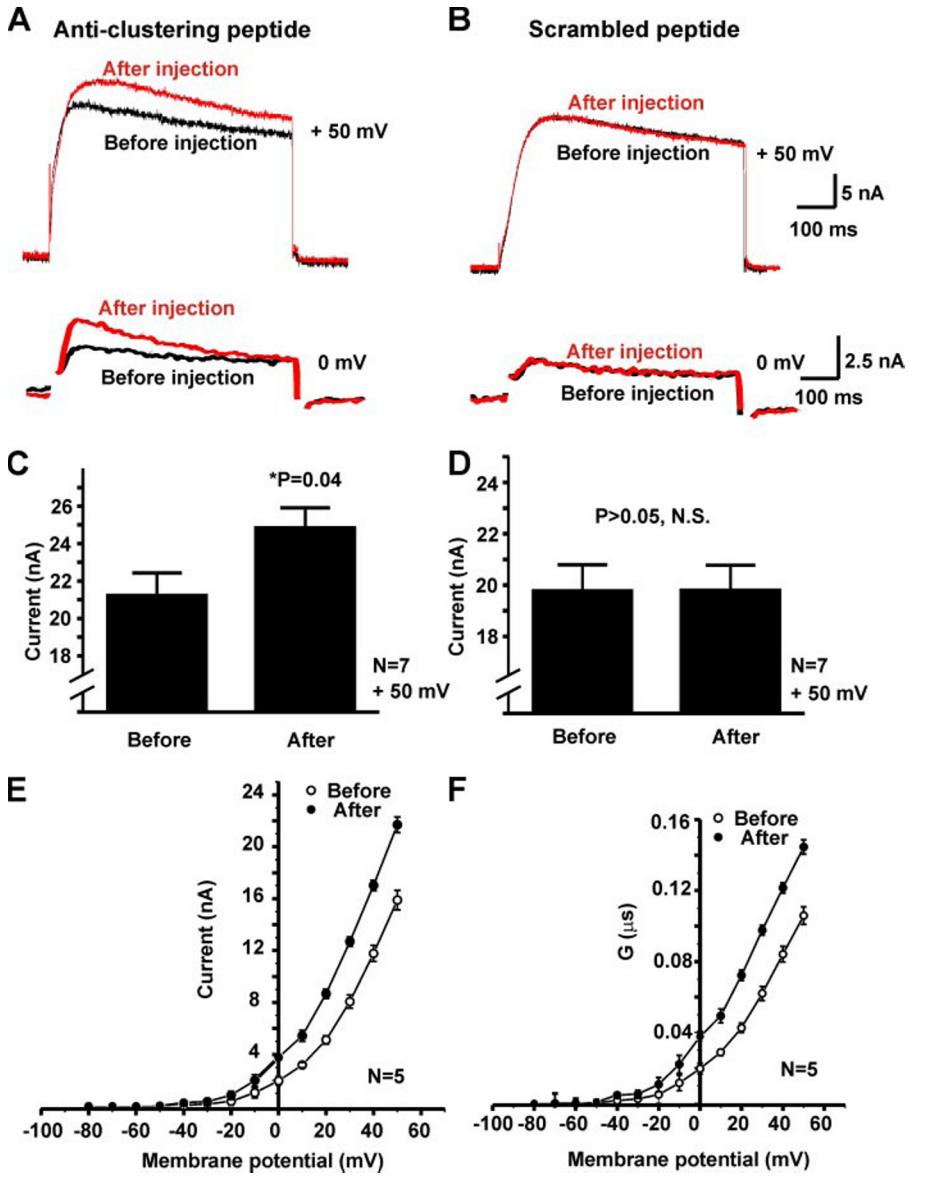

FIGURE 6. **Effects of injecting anti-clustering peptide on potassium currents in isolated bag cell neurons.** *A* and *B*, outward currents in bag cell neurons before and after injection of anti-clustering peptide (*A*) or control peptide (*B*). The *traces* represent single-microelectrode voltage clamp recordings from a bag cell neuron maintained in primary culture. The holding potential was maintained at −40 mV, the outward current was evoked by a depolarizing pulse to +50 mV or 0 mV. *C* and *D*, summary of the effect of anti-clustering peptide (*C*) and control peptide (*D*) on net outward current measured at +50 mV. The data are expressed as the means ± S.E. The *asterisk* indicates a significant difference from control at $p < 0.05$. *E*, current-voltage relationships for single electrode voltage clamp recording on isolated bag cell neurons. The currents were recorded with or without peptide in injection solution and evoked by depolarizing the membrane from a holding potential of −40 mV to test potentials from −40 to +50 mV ($n = 5$). *F*, conductance voltage relationship for peak I_K currents recorded from before and after microinjection of the anti-clustering peptide. The data shown are the means ± S.E. ($n = 5$).

steady state inactivation of *Aplysia* Kv2.1 (8), Kv2.1 currents are strongly represented in the voltage-dependent K^+ currents evoked from this holding potential. Injections of anti-clustering peptide were made after at least 5 min of stable recording. Within 5 min of injection of this peptide, potassium current was found to increase at all test potentials, giving an ~ 50% increase in current at 0 mV and an ~15–20% increase at +50 mV ($n = 7$; Fig. 6, *A*, *C*, and *E*). In contrast, no change in evoked currents was detected on injection of the control 12-amino acid peptide corresponding to the S1-S2 region (Fig. 6, *B*, *D*, and *F*).

Fig. 6*E* shows the mean current-voltage relationships for K^+ currents recorded before and after injecting the anti-clustering peptide using sharp electrode voltage clamp recording from isolated bag cell neurons. K^+ currents were evoked by depolarizing the membrane potential from a holding potential of −40 mV. We also calculated conductance-voltage relations by dividing current by the electrochemical driving force ($I_K/(V_m - E_K)$). Fig. 6*F* demonstrates that, following injection of the anti-clustering peptide, there is a greater increase in K^+ currents at negative potentials (−40 to 0 mV) than at more positive potentials. This is consistent with a shift in voltage dependence of activation toward negative potentials, although the true values for $V_{½}$ of activation before and after injection were not calculated because, as found previously for bag cell neurons (26) and for *Aplysia* Kv2.1-expressing oocytes (8), full activation of K^+ currents does not occur at potentials negative to +60 mV.

We found no statistically significant differences in the rates of activation or the degree of inactivation of K^+ currents following injection of the anti-clustering peptide. In response to a command pulse to +50 mV, the time to reach 66% of peak current amplitude was 44.7 ± 3.6 and 46.3 ± 4.1 ms before and after injection of the peptide, respectively ($n = 5$, no significant difference). The degree of inactivation ($I_{steady\ state}/I_{peak}$) during pulses at +50 mV was 0.16 ± 0.03 and 0.16 ± 0.02 before and after injection, respectively ($n = 4$, no significant difference). A statistically significant difference in degree of inactivation was, however, observed at 0 mV (0.15 ± 0.02 *versus* 0.25 ± 0.02, before and after injection of the peptide, respectively ($n = 4$, $p < 0.02$).

To test the effects of the anti-clustering peptide on the characteristics of action potentials in current clamp recordings, isolated neurons were subjected to 10 depolarizing current pulses (250 ms, 0.25 nA) applied at a frequency of 1 Hz. This pattern of stimulation produces progressive broadening of action potentials (Fig. 7, *A* and *C*), which results in major part from the inactivation of potassium currents during the repeated depolarizations (8, 26). Within 5–10 min of injection of the anti-

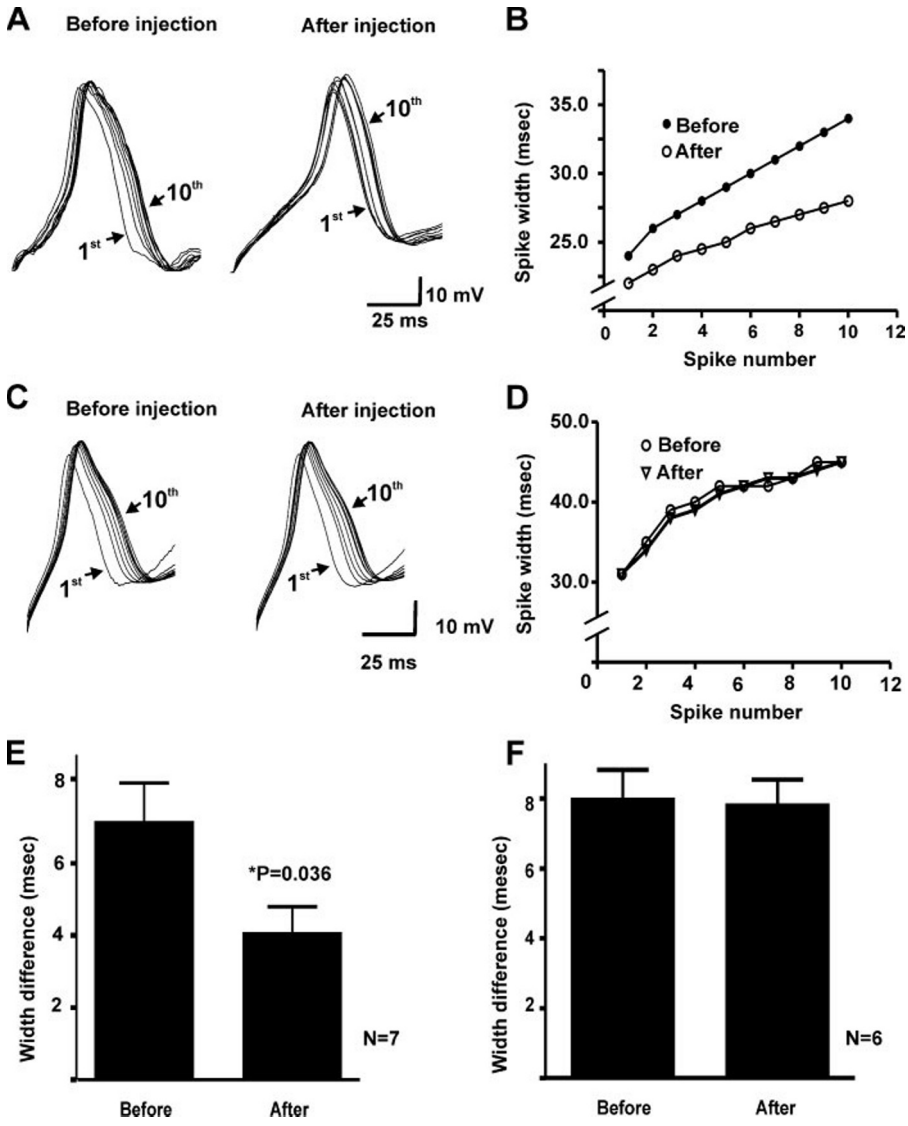

FIGURE 7. **Effects of anti-clustering peptide and control peptide on action potentials in bag cell neurons.** Superimposed traces of action potentials evoked by repetitive stimulation of an isolated bag cell neuron maintained in primary culture. Ten depolarizing current pulses (250 ms, 0.25 nA) were applied at a frequency of 1 Hz. Each successive evoked action potential is wider than the previous action potential. Action potentials were evoked from a resting potential of −60 mV. *A*, after injection of the anti-clustering peptide into the bag cell neuron, the action potentials are narrower, and less broadening occurs during the train of 10 pulses. *B*, quantification of the width of successive action potentials, plotted as a function of pulse number in the train, before and after injection of the anti-clustering peptide. Action potential width was measured at a potential midway between the resting potential and the peak of the action potential. *C*, after injection of the control peptide into the bag cell neurons as in *A*, the width of action potentials and the degree of spike broadening are unchanged. *D*, quantification of the width of successive action potentials, plotted as a function of pulse number in the train, before and after injection of the control peptide. *E* and *F*, mean data for the amount of broadening of action potentials before and after injection of the anti-clustering peptide (*E*) or control peptide (*F*). The data are expressed as the means ± S.E. The *asterisk* indicates a significant difference from control at $p < 0.05$.

clustering peptide, the width of the first action potential in such a train became reduced relative to that prior to injection, and subsequent pulses in the train produced significantly less broadening of evoked action potentials ($n = 7$; Fig. 7, *A* and *B*). The change in action potential shape was quantified by determining the difference between the width of the first and tenth action potentials measured at a voltage corresponding to the mid-point between the resting potential and the peak of the action potential (Fig. 7, *B* and *E*). In contrast, injection of the control peptide produced no significant change in the width of the first action potential or in the degree of broadening with repeated stimulation at 1 Hz (Fig. 7, *C*, *D*, and *F*). To control for possible variations in action potential characteristics between the cells used for anti-clustering and control peptide injections, we measured action potential widths, heights, and resting potentials in the two groups. The mean first action potential widths before injections were 25.50 ± 1.13 and 25.00 ± 0.7 ms in the control and experimental groups, respectively. Action potential amplitudes were 49.75 ± 2.71 and 49.00 ± 1.43 mV, and resting membrane potentials were −56.4 ± 1.5 and −55.26 ± 1.4 mV, respectively, in the two groups ($n = 7$).

Because injection of the anti-clustering peptide produces an increase in potassium currents with little change in macroscopic rates of activation or inactivation, we carried out computer simulations to determine whether a reduced rate of action potential broadening is consistent with a simple increase in current. We used a previously described model of *Aplysia* Kv2.1 gating (8) in a simplified bag cell neuron model that incorporated, in addition to *Aplysia* Kv2.1, a calcium current, one noninactivating voltage-dependent potassium current and a leakage conductance. As described previously (8), inactivation of *Aplysia* Kv2.1 during 10 consecutive depolarizing current pulses provides action potential broadening (Fig. 8*A*). Increasing *Aplysia* Kv2.1 current either by increasing its maximal conductance or by introducing a negative shift in its voltage dependence of activation (Fig. 8*B*) substantially reduced broadening during the 10 depolarizing current pulses (Fig. 8, *A* and *C*). This reduction in broadening occurs because of the effect on Kv2.1 current on action potential shape. The increase in Kv2.1 current reduces the width and height of action potentials, and, as a result, less voltage-dependent inactivation of this current occurs during repetitive stimulation.

DISCUSSION

Different potassium channels have been found to have distinct patterns of spatial localization in neurons (27). In part, such compartmentalization serves to control the excitability of

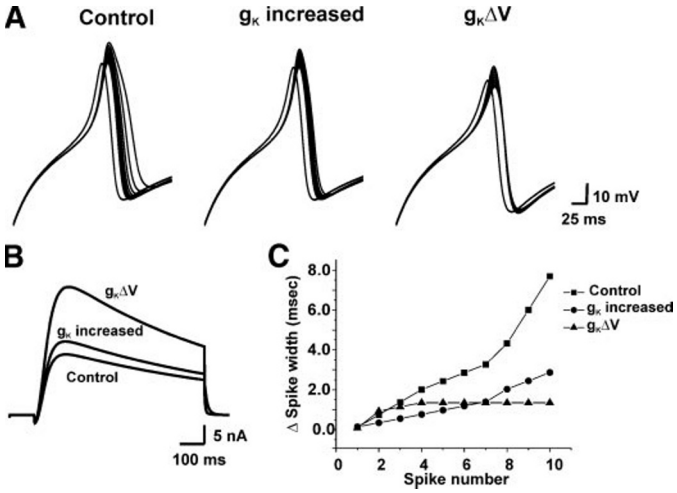

FIGURE 8. **Computer simulations of action potential broadening in a simplified neuronal model incorporating the Aplysia Kv2.1 channel with kinetic parameters as described by Quattrocki *et al.* (8).** *A*, 10 superimposed action potentials evoked by a 100-ms, 1.2-nA current pulse applied at a frequency of 4 Hz. In the center panel the value of the maximal Kv2.1 conductance (g_K) was increased from 1.5 to 1.8 μS. In the *right panel*, Kv2.1 current was increased by introducing a 10-mV negative shift in voltage of activation ($g_K\Delta V$). *B*, numerical simulations of total current evoked under voltage clamp by 700-ms depolarizations from a holding potential of −40 to 0 mV under the conditions described in *A*. *C*, quantification of the change in width of successive action potentials, plotted as a function of pulse number in the train in the three conditions. Action potential width was measured at a potential midway between the resting potential and the peak of the action potential and subtracted from the width of the first action potential.

different parts of the cell. For example, the A-type channel Kv1.4 is primarily along axonal membranes (28), whereas in hippocampal and cortical neurons Kv2.1 is found primarily on soma and proximal dendrites, where it may control impulse flow into and out of the soma (4, 5, 10, 29–33). Specific patterns of spatial localization may, however, also serve to couple potassium channels to intracellular signaling pathways. In the case of mammalian Kv2.1, the ring-shaped clusters in the plasma membrane may be closely linked to subsurface cisternae and co-localized with ryanodine receptors (32, 34), suggesting that the modulation of Kv2.1 channels may be associated with the regulation of intracellular calcium stores.

We have found that plasma membrane immunoreactivity of the Kv2.1 channel in the bag cell neurons of *Aplysia* is, like that of mammalian neurons (10), localized to very dense, discrete clusters on the somata. These very distinctive donut- or C-shaped clusters are also present on proximal dendrites and at the terminals of bag cell neurons. We have also shown that the formation and dissolution of these clusters is regulated by physiological patterns of neuronal activity and that it is associated with changes in the gating properties of the Kv2.1 channel.

Although we cannot definitively exclude the possibility that some of the changes in distribution that we observed are associated with rapid changes in surface expression or internalization, it is likely that major observed changes result from clustering/unclustering within the plasma membrane. For example, the dissolution of clusters in response to injection of the anti-clustering peptide is unlikely to result from internalization because this peptide produces an increase in current. Conversely, elevations of cAMP, which increase cluster number, produce a decrease in current (9, 25, 26). Moreover, the anti APKv2.1 antibody was raised against an extracellular epitope, and the neurons were not permeabilized. Finally internalization into intracellular organelles would be expected to produce a punctate pattern of staining, corresponding to internal organelles, rather a diffuse staining pattern such as was seen in the peptide-injected cells.

When clustered, the voltage of activation of Kv2.1 appears to be shifted to more positive potentials than when channel localization has been dispersed by intracellular injection of a peptide derived from the clustering domain located in the C terminus of the channel. A similar shift in the conductance-voltage relations of rat Kv2.1 has been found in response to glutamate application or other stimuli that cause unclustering and dephosphorylation of the rat Kv2.1 (6, 33). It is not clear, however, whether the shift in voltage dependence of activation is a direct consequence of clustering or whether the change in spatial distribution produces a different pattern of post-translational modification at sites on the Kv2.1 protein that are not related to channel clustering.

In the bag cell neurons, physiological stimulation of the connective nerve input elevates cyclic AMP levels (16) and triggers an afterdischarge that we have now shown is associated with an increase in Kv2.1 channel clustering. The changes in the shape of action potentials at the onset of afterdischarge are entirely consistent with those expected from either a decrease in amplitude or a positive shift in voltage dependence of activation of Kv2.1 and are the reverse of those observed on injection of the anti-clustering peptide. In particular, the width of action potentials is substantially broadened, and the degree of frequency-dependent broadening is increased at the onset of afterdischarge (35). These broadened action potentials allow impulses that are generated at the distal tips of bag cell neurites in the pleuroabdominal connective to propagate through the proximal neurites and somata to invade the bag cell network in the contralateral cluster (16). In this respect, the function of Kv2.1 in bag cell neurons resembles that proposed for mammalian Kv2.1, namely to regulate the ability of action potentials generated at distal locations to invade the somata and proximal neurites (33).

One of the puzzles related to potassium channels is the high degree of conservation of different potassium channel families across evolution. This conservation appears to be unrelated to the specific electrical characteristics of each channel family, which can vary across species. For example the kinetic behavior of *Aplysia* Kv2.1, which undergoes relatively rapid cumulative inactivation with repeated depolarization, is quite distinct from that of mammalian Kv2.1 channels that have been investigated (36). The latter typically undergo little inactivation during depolarizations lasting several seconds. Moreover, *Aplysia* Kv2.1 channels contribute to repolarization of individual action potentials (8), whereas repetitive firing is required to activate Kv2.1 currents in mammalian neurons (4). Our finding that Kv2.1 channels in *Aplysia* undergo dynamic clustering and unclustering during physiologically induced changes in neuronal excitability suggests that it may be this aspect of channel function, rather than its specific gating behavior, that has led to the conservation of the Kv2.1 channel through evolution.

REFERENCES

1. Pak, M. D., Covarrubias, M., Ratcliffe, A., and Salkoff, L. (1991) *J. Neurosci.* **11,** 869–880
2. Frech, G. C., VanDongen, A. M., Schuster, G., Brown, A. M., and Joho, R. H. (1989) *Nature* **340,** 642–645
3. Blaine, J. T., and Ribera, A. B. (2001) *J. Neurosci.* **21,** 1473–1480
4. Du, J., Haak, L. L., Phillips-Tansey, E., Russell, J. T., and McBain, C. J. (2000) *J. Physiol.* (*Lond.*) **522,** 19–31
5. Misonou, H., Mohapatra, D. P., Park, E. W., Leung, V., Zhen, D., Misonou, K., Anderson, A. E., and Trimmer, J. S. (2004) *Nat. Neurosci.* **7,** 711–718
6. Park, K. S., Mohapatra, D. P., Misonou, H., and Trimmer, J. S. (2006) *Science* **313,** 976–979
7. Tsunoda, S., and Salkoff, L. (1995) *J. Neurosci.* **15,** 5209–5221
8. Quattrocki, E. A., Marshall, J., and Kaczmarek, L. K. (1994) *Neuron* **12,** 73–86
9. Kaczmarek, L. K., and Strumwasser, F. (1981) *J. Neurosci.* **1,** 626–634
10. Lim, S. T., Antonucci, D. E., Scannevin, R. H., and Trimmer, J. S. (2000) *Neuron* **25,** 385–397
11. Conn, P. J., and Kaczmarek, L. K. (1989) *Mol. Neurobiol.* **3,** 237–273
12. Kupfermann, I., and Kandel, E. R. (1970) *J. Neurophysiol.* **33,** 865–876
13. Chun, J. Y., Korner, J., Kreiner, T., Scheller, R. H., and Axel, R. (1994) *Neuron* **12,** 831–844
14. Arch, S., and Berry, R. W. (1989) *Brain Res. Brain Res. Rev.* **14,** 181–201
15. Nagle, G. T., de Jong-Brink, M., Painter, S. D., Bergamin-Sassen, M. M., Blankenship, J. E., and Kurosky, A. (1990) *J. Biol. Chem.* **265,** 22329–22335
16. Kaczmarek, L. K., Jennings, K., and Strumwasser, F. (1978) *Proc. Natl. Acad. Sci. U. S. A.* **75,** 5200–5204
17. Dudek, F. E., and Blankenship, J. E. (1976) *Science* **192,** 1009–1010
18. White, B. H., and Kaczmarek, L. K. (1997) *J. Neurosci.* **17,** 1582–1595
19. Kaczmarek, L. K., Finbow, M., Revel, J. P., and Strumwasser, F. (1979) *J. Neurobiol.* **10,** 535–550
20. Jonas, E. A., Knox, R. J., Kaczmarek, L. K., Schwartz, J. H., and Solomon, D. H. (1996) *J. Neurosci.* **16,** 1645–1658
21. Wilson, W. A., and Goldner, M. M. (1975) *J. Neurobiol.* **6,** 411–422
22. Chiu, A. Y., and Strumwasser, F. (1981) *J. Neurosci.* **1,** 812–826
23. Wayne, N. L., Kim, Y. J., and Yong-Montenegro, R. J. (1998) *Gen. Comp. Endocrinol.* **109,** 356–365
24. Azhderian, E. M., Hefner, D., Lin, C. H., Kaczmarek, L. K., and Forscher, P. (1994) *Neuron* **12,** 1223–1233
25. Loechner, K. J., and Kaczmarek, L. K. (1990) *Brain Res.* **532,** 1–6
26. Kaczmarek, L. K., and Strumwasser, F. (1984) *J. Neurophysiol.* **52,** 340–349
27. Trimmer, J. S., and Rhodes, K. J. (2004) *Annu. Rev. Physiol.* **66,** 477–519
28. Sheng, M., Tsaur, M. L., Jan, Y. N., and Jan, L. Y. (1992) *Neuron* **9,** 271–284
29. Trimmer, J. S., Cooperman, S. S., Agnew, W. S., and Mandel, G. (1990) *Dev. Biol.* **142,** 360–367
30. Tsuk, S., Michaelevski, I., Bentley, G. N., Joho, R. H., Chikvashvili, D., and Lotan, I. (2005) *Mol. Pharmacol.* **67,** 480–488
31. Scannevin, R. H., Murakoshi, H., Rhodes, K. J., and Trimmer, J. S. (1996) *J. Cell Biol.* **135,** 1619–1632
32. Du, J., Tao-Cheng, J. H., Zerfas, P., and McBain, C. J. (1998) *Neuroscience* **84,** 37–48
33. Misonou, H., Mohapatra, D. P., and Trimmer, J. S. (2005) *Neurotoxicology* **26,** 743–752
34. Antonucci, D. E., Lim, S. T., Vassanelli, S., and Trimmer, J. S. (2001) *Neuroscience* **108,** 69–81
35. Kaczmarek, L. K., Jennings, K. R., and Strumwasser, F. (1982) *Brain Res.* **238,** 105–115
36. Ju, M., Stevens, L., Leadbitter, E., and Wray, D. (2003) *J. Biol. Chem.* **278,** 12769–12778